

# Resonant Inelastic X-ray Scattering on Spin-Orbit Coupled Insulating Iridates

Luuk J.P. Ament<sup>1</sup>, Giniyat Khaliullin<sup>2</sup>, Jeroen van den Brink<sup>3</sup>

<sup>1</sup>*Institute-Lorentz for Theoretical Physics, Universiteit Leiden, 2300 RA Leiden, The Netherlands*

<sup>2</sup>*Max-Planck-Institut für Festkörperforschung, Heisenbergstrasse 1, D-70569 Stuttgart, Germany and*

<sup>3</sup>*Leibniz-Institute for Solid State and Materials Research Dresden, D-01171 Dresden, Germany*

(Dated: August 31, 2010)

We determine how the elementary excitations of iridium-oxide materials, which are dominated by a strong relativistic spin-orbit coupling, appear in Resonant Inelastic X-ray Scattering (RIXS). Whereas the RIXS spectral weight at the  $L_2$  x-ray edge vanishes, we find it to be strong at the  $L_3$ -edge. Applying this to  $\text{Sr}_2\text{IrO}_4$ , we observe that RIXS, besides being sensitive to local doublet to quartet transitions, meticulously maps out the strongly dispersive delocalized excitations of the low-lying spin-orbit doublets.

PACS numbers: 78.70.Ck, 75.30.Et, 75.25.Dk, 71.70.Ej

Materials containing ions with an orbital degeneracy show a plethora of physical effects related to the spontaneous lifting of this degeneracy [1]. The two degeneracy-breaking mechanisms in Mott insulators traditionally considered are the cooperative Jahn-Teller effect [2], involving a change in lattice symmetry, and the superexchange interactions [3], intertwining long-range ordering of orbital and magnetic degrees of freedom. A third and less explored possibility exists in systems containing heavy ions, where strong relativistic spin-orbit coupling dominates the spin-orbital physics [4].

The strong spin-orbit interaction can cause entirely new kinds of ordering that are of topological nature. This was recently proposed for certain iridium-oxides [5, 6], members of a large family of iridium-based materials.  $\text{Na}_2\text{IrO}_3$ , for instance, is predicted to be a topological insulator exhibiting the quantum spin Hall effect at room temperature [5]. The topologically non-trivial state arises from the presence of complex hopping integrals, resulting from the unquenched iridium orbital moment. This system can also be described in terms of a Mott insulator, with interactions between the effective iridium spin-orbital degrees of freedom governed by the Kitaev-Heisenberg model [7–9]. In the pyrochlore iridates  $\text{A}_2\text{Ir}_2\text{O}_7$  (where A is a 3+ ion), a quantum phase transition from a topological band insulator to a topological Mott insulator has been proposed as a function of the electron-electron interaction strength [6, 10, 11].

To establish whether and how such novel phases are realized in iridium oxides it is essential to probe and understand their spin-orbital ordering and related elementary excitations. In this context it is advantageous to consider the structurally less complicated, single-layer iridium perovskite  $\text{Sr}_2\text{IrO}_4$ . This material is in many respects the analog of the high- $T_c$  cuprate parent compound  $\text{La}_2\text{CuO}_4$  [8]. Structurally it is identical, with the obvious difference that the Ir  $5d$  valence electrons are, as opposed to the Cu  $3d$  electrons, very strongly spin-orbit coupled. The similarity cuts deeper, however, as the low energy sector of the iridates is spanned by local spin-orbit

doublets with an effective spin of  $1/2$ , which reside on a square lattice and interact via superexchange – a close analogy with the undoped cuprates. This observation motivates doping studies of  $\text{Sr}_2\text{IrO}_4$  searching for superconductivity [12, 13]. Experimentally, however, far less is known about the microscopic ordering and excitations in iridates than in cuprates. Inelastic neutron scattering, which can in principle reveal such properties, is not possible because Ir is a strong neutron absorber [14] and, moreover, crystals presently available tend to be tiny. As a consequence not even the interaction strength between the effective spins in the simplest iridium-oxides is established: estimates for  $\text{Sr}_2\text{IrO}_4$ , for instance, range from  $\sim 50$  meV [8] to  $\sim 110$  meV [15].

In this Letter we show that while for iridates neutron scattering falls short, photon-in photon-out scattering in the form of resonant inelastic x-ray scattering (RIXS) [16] fills the void: RIXS at the iridium  $L$ -edge offers direct access to the excitation spectrum across the Brillouin zone, enabling one to measure the dispersion of elementary magnetic excitations. Besides the low energy magnons related to long-range order of the doublets, RIXS will also reveal the dynamics of higher energy, doublet-to-quartet, spin-orbit excitations. This allows to directly test theoretical models for the excitation spectra and extract accurate values of the superexchange and spin-orbit coupling constants  $J$  and  $\lambda$ , respectively.

*Ir<sup>4+</sup> ionic ground state.* — In the iridium-oxides  $\text{Ir}^{4+}$  ions are located in octahedra of oxygen ions, splitting the  $5d$  levels by  $\sim 3$  eV into  $e_g$  and  $t_{2g}$  orbitals [17]. Because this crystal field splitting is an order of magnitude larger than the spin-orbit coupling  $\lambda$ , the  $t_{2g}$  levels do not hybridize much with the  $e_g$  orbitals, and a  $t_{2g}^5$  configuration is established [18]. The symmetry of the  $t_{2g}^5$  ground state is in principle governed by three factors: superexchange interactions, additional lattice-induced crystal field splittings, and relativistic spin-orbit coupling [19]. The superexchange  $J$  [8] is estimated to be about an order of magnitude smaller than  $\lambda \approx 0.4$  eV [20]. An elongation of the octahedra along the  $z$  axis [21] favors a ground

state where the hole is in the  $xy$  orbital. But experimental data strongly favor the spin-orbit coupling scenario over the lattice splitting scenario, however [4, 18].

The orbital degree of freedom of the hole can be described by an effective angular momentum  $l = 1$ , related to the true orbital angular momentum by  $\mathbf{l} = -\mathbf{L}$  [22]. The orbital eigenstates of  $l_z$  are described by the annihilation operators  $d_{0,\pm 1}$ , defined in terms of the real  $t_{2g}$  wave functions by the relations  $d_{yz} = -(d_1 - d_{-1})/\sqrt{2}$ ,  $d_{zx} = i(d_1 + d_{-1})/\sqrt{2}$ ,  $d_{xy} = d_0$ . When the spin-orbit coupling term is projected to the  $t_{2g}$  subspace, it becomes  $-\lambda \mathbf{l} \cdot \mathbf{S}$ . Tetragonal lattice distortions can also be included, and the Hamiltonian for a single Ir ion is [8]  $H = -\lambda \mathbf{l} \cdot \mathbf{S} - \Delta l_z^2$ , with  $\Delta > 0$  for elongation along the  $z$  axis. The six eigenstates group into three Kramers doublets, described by the fermions  $f$ ,  $g$  and  $h$  with annihilation operators

$$\begin{aligned} f_\uparrow &= \sin \theta d_{0\uparrow} - \cos \theta d_{1\downarrow}, & g_\uparrow &= d_{1\uparrow}, \\ f_\downarrow &= \cos \theta d_{-1\uparrow} - \sin \theta d_{0\downarrow}, & g_\downarrow &= d_{-1\downarrow}, \\ h_\uparrow &= \cos \theta d_{0\uparrow} + \sin \theta d_{1\downarrow}, \\ h_\downarrow &= \cos \theta d_{0\downarrow} + \sin \theta d_{-1\uparrow}, \end{aligned} \quad (1)$$

and with energies  $\omega_f = \lambda/(\sqrt{2} \tan \theta)$ ,  $\omega_g = -\Delta - \lambda/2$  and  $\omega_h = -(\lambda \tan \theta)/\sqrt{2}$ , where  $\tan 2\theta = 2\sqrt{2}\lambda/(\lambda - 2\Delta)$ . For  $\Delta = 0$ , which corresponds to the cubic, isotropic situation  $\sin \theta = \sqrt{1/3}$  and  $\cos \theta = \sqrt{2/3}$ . For  $\lambda/\Delta \ll 1$ , the hole's ground state doublet is  $\{|xy \uparrow\rangle, |xy \downarrow\rangle\}$ . For  $\lambda/\Delta \gg 1$ , the eigenstates are characterized by the total effective angular momentum  $\mathbf{J}_{\text{eff}} = \mathbf{l} + \mathbf{S}$ . In the ground state, the hole occupies the  $f$  doublet ( $J_{\text{eff}} = 1/2$ ), which is separated by an energy of  $3\lambda/2$  from the  $J_{\text{eff}} = 3/2$  quartet, which splits into the  $g$  and  $h$  doublets.

The remaining, two-fold ground state degeneracy cannot be removed by Jahn-Teller distortions because the two states in the ground state Kramers doublet have exactly the same charge distribution. Superexchange coupling, however, is present in all iridates, and couples the local doublets, thus dictating the low energy collective dynamics of the material.

**RIXS cross section.** — Resonant Inelastic X-ray Scattering is particularly suited to probe higher energy magnetic excitations and dispersions, as demonstrated in the cuprates [23–26]. The recent increase in brilliance of the new generation synchrotron X-ray sources allows for spectra with tremendous resolving powers, enough to resolve dispersion up to a few tens of meV. In RIXS [16, 27], a photon with momentum  $\hbar \mathbf{k}$ , energy  $\omega_{\mathbf{k}}$  and polarization  $\epsilon$  is scattered to  $\hbar \mathbf{k}'$ ,  $\omega_{\mathbf{k}'}$  and  $\epsilon'$ , losing momentum  $\hbar \mathbf{q} = \hbar \mathbf{k} - \hbar \mathbf{k}'$  and energy  $\omega = \omega_{\mathbf{k}} - \omega_{\mathbf{k}'}$  to the sample.  $\omega_{\mathbf{k}}$  is tuned to a certain atomic resonance of the material under study, greatly enhancing the scattering cross section. In our case, that will be the Ir  $L$ -edge: the  $2p$  core electron is excited into the empty  $5d t_{2g}$  state. After a very short time, another electron from the  $t_{2g}$  levels can fall back to the core hole under the emission of an outgoing

X-ray. The system is left in an excited state, whose energy and momentum are taken from the scattered X-ray photon, which is measured.

The RIXS cross section is described by the Kramers-Heisenberg equation [28], where the photon absorption and subsequent emission are governed by the dipole operator  $\mathcal{D} = \sum_{\mathbf{R}} e^{i\mathbf{k} \cdot \mathbf{R}} \mathbf{r} \cdot \epsilon$  acting on all electrons of an  $\text{Ir}^{4+}$  ion at site  $\mathbf{R}$ . The phonon polarization is  $\epsilon$ .

The intermediate state has a filled shell ( $5d t_{2g}^6$ ), so the dominant multiplet effect comes from the core orbital's spin-orbit coupling  $\Lambda$ : the  $2p$  core states split into  $J = 1/2$  (the  $L_2$  edge) and  $J = 3/2$  states (the  $L_3$  edge). Since the  $L_2$  and the  $L_3$  edge are separated by 1.6 keV [4], their interference is negligible, given the much smaller lifetime broadening of a few eV [29]. Because the  $2p$  core states have the same angular momenta as the  $5d t_{2g}$  states, we can describe them with the three fermions  $F$ ,  $G$  and  $H$ , analogous to Eq. (1), where we replace  $(d_{yz}, d_{zx}, d_{xy})$  by  $(p_x, p_y, p_z)$  and the parameters  $\lambda$ ,  $\Delta$  and  $\theta$  by  $\Lambda$ ,  $\delta$  and  $\Theta$ . The tetragonal distortion  $\delta$  is expected to be very small for the deep  $2p$  core states.

The lifetime broadening at the Ir  $L$  edge is still quite large compared to the dynamics of the  $5d$  electrons [18, 29]. Therefore, we make the fast collision approximation  $E_i + \hbar \omega_{\mathbf{k}} - E_n + i\Gamma \approx i\Gamma$  [30]. The sum over  $n$  in the Kramers-Heisenberg equation can be performed, and comprises the core states of either the  $L_2$  or the  $L_3$  edge. In second quantization, the dipole operators are  $\mathbf{r} \cdot \epsilon = \sum_{\alpha, \beta, \sigma} \langle 5d_\alpha | \mathbf{r} | 2p_\beta \rangle \cdot \epsilon d_{\alpha\sigma}^\dagger p_{\beta\sigma} + \text{h.c.}$  which can be denoted as  $(D_2 + D_3) + \text{h.c.}$ , where  $D_{2,3}$  are the local dipole transition operators for the  $L_2$  and  $L_3$  edge, respectively. The RIXS amplitude becomes  $A_{\mathbf{q}} \propto \langle f | \sum_{\mathbf{R}} e^{i\mathbf{q} \cdot \mathbf{R}} [D^\dagger(\epsilon'^*) D(\epsilon)]_{\mathbf{R}} | 0 \rangle$ , where  $\mathbf{R}$  runs over all Ir sites and the RIXS intensity  $I_{\mathbf{q}}(\omega) = \sum_f |A_{\mathbf{q}}|^2 \delta(\omega - E_f)$ . We rewrite the inelastic scattering operator as

$$\begin{aligned} D^\dagger D = \sum_{\sigma \in \{\uparrow, \downarrow\}} & \left[ B_{\sigma\sigma}^{ff} f_\sigma^\dagger f_\sigma + B_{\sigma\sigma}^{ff} f_\sigma^\dagger f_{\bar{\sigma}} + B_{\sigma\sigma}^{fg} f_\sigma^\dagger g_\sigma \right. \\ & \left. + B_{\sigma\sigma}^{fg} f_\sigma^\dagger g_{\bar{\sigma}} + B_{\sigma\sigma}^{fh} f_\sigma^\dagger h_\sigma + B_{\sigma\sigma}^{fh} f_\sigma^\dagger h_{\bar{\sigma}} \right]. \end{aligned} \quad (2)$$

Integrating out the core hole degree of freedom one obtains at the  $L_2$  edge the intra-doublet scattering matrix elements  $B_{\sigma\sigma}^{ff} = -\sin^2(\theta - \Theta) \epsilon_\sigma'^* \epsilon_{\bar{\sigma}}$  and  $B_{\sigma\sigma}^{ff} = 0$ . The doublet-quartet excitation matrix elements of the spin-orbit multiplet are  $B_{\sigma\sigma}^{fg} = \sin(\theta - \Theta) \cos \Theta \epsilon_\sigma'^* \epsilon_{\bar{\sigma}}$ ,  $B_{\sigma\sigma}^{fg} = -(-1)^\sigma \sin(\theta - \Theta) \sin \Theta \epsilon_\sigma'^* \epsilon_{\bar{\sigma}}$ ,  $B_{\sigma\sigma}^{fh} = -\frac{1}{2}(-1)^\sigma \sin 2(\theta - \Theta) \epsilon_\sigma'^* \epsilon_{\bar{\sigma}}$  and  $B_{\sigma\sigma}^{fh} = 0$ , where  $(-1)^\sigma$  is 1 for  $\sigma = \uparrow$  and  $-1$  for  $\sigma = \downarrow$ . Further,  $\epsilon_\uparrow = \epsilon_+$  and  $\epsilon_\downarrow = \epsilon_-$ , with  $\epsilon_\pm = (\epsilon_x \pm i\epsilon_y)/\sqrt{2}$ . In the case of dominant spin-orbit coupling,  $\theta = \Theta$ . Since all matrix elements at the  $L_2$  edge are proportional to  $\sin(\theta - \Theta)$ , the inelastic scattering intensity vanishes completely in this case, in addition to a vanishing of the elastic intensity [4].

At the  $L_3$  edge, however, RIXS is fully allowed. The matrix elements are:  $B_{\sigma\sigma}^{ff} = -\sin^2 \theta \epsilon_\sigma'^* \epsilon_{\bar{\sigma}} - \cos^2(\theta -$

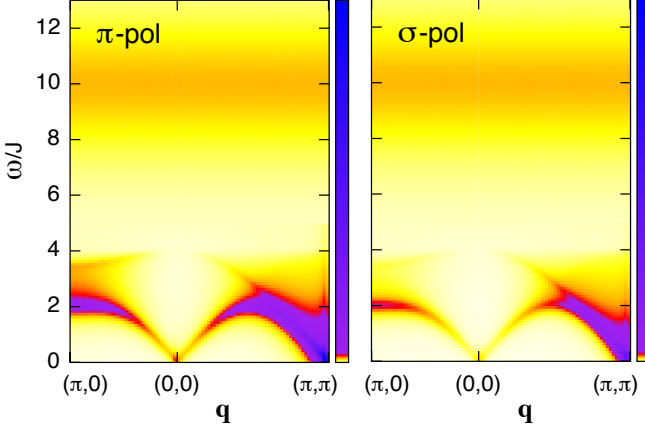


FIG. 1: (Color online.) RIXS spectra of  $\text{Sr}_2\text{IrO}_4$  at the Ir  $L_3$   $t_{2g}$  edge. The left panel shows the spectrum for incoming  $\pi$  polarization, and the right one for incoming  $\sigma$  polarization. The outgoing polarization is not measured. The intra-doublet excitations are broadened by  $J/10$ .

$\Theta)\epsilon'_{\sigma}^*\epsilon_{\sigma} - \cos^2\theta \epsilon'_{\sigma}^*\epsilon_{\sigma}$  and  $B_{\sigma\sigma}^{ff} = \frac{1}{2}(-1)^{\sigma} \sin 2\theta (\epsilon'_{\sigma}^*\epsilon_{\sigma} - \epsilon'_{\sigma}^*\epsilon_{\sigma})$  for the intra-doublet ones, and  $B_{\sigma\sigma}^{fg} = \cos(\theta - \Theta) \sin \Theta \epsilon'_{\sigma}^*\epsilon_{\sigma}$ ,  $B_{\sigma\sigma}^{fg} = (-1)^{\sigma} \cos(\theta - \Theta) \cos \Theta \epsilon'_{\sigma}^*\epsilon_{\sigma}$ ,  $B_{\sigma\sigma}^{fh} = \frac{1}{2}(-1)^{\sigma} [\sin 2(\theta - \Theta) \epsilon'_{\sigma}^*\epsilon_{\sigma} - \sin 2\theta (\epsilon'_{\sigma}^*\epsilon_{\sigma} - \epsilon'_{\sigma}^*\epsilon_{\sigma})]$ ,  $B_{\sigma\sigma}^{fh} = -\sin^2\theta \epsilon'_{\sigma}^*\epsilon_{\sigma} - \cos^2\theta \epsilon'_{\sigma}^*\epsilon_{\sigma}$  for the doublet-quartet excitations. For excitations within the  $J_{\text{eff}} = 1/2$  doublet, the scattering operator can be rewritten in terms of the effective angular momentum operator, which in the limit  $\Delta/\lambda \ll 1$  takes the particularly simple form  $D_3^{\dagger}D_3 = \frac{2}{3}(\epsilon' \cdot \epsilon \mathbb{1} + \mathbf{P} \cdot \mathbf{J}_{\text{eff}})$ , where  $P_x = i(\epsilon'_y \epsilon_z - \epsilon'_z \epsilon_y)$  and its cyclic permutations  $P_{y,z}$  are polarization factors. Here, the first term corresponds to elastic scattering while the  $\mathbf{P} \cdot \mathbf{J}_{\text{eff}}$  term gives rise to inelastic scattering.

*RIXS on  $\text{Sr}_2\text{IrO}_4$ .* — Up to this point, the discussion is general and applies to all materials with an  $\text{Ir}^{4+}$  ion in an octahedral crystal field. Calculation of the RIXS spectra for a particular iridate is straightforward given the Hamiltonian that captures the interactions between the Ir degrees of freedom. In  $\text{Sr}_2\text{IrO}_4$  the effective low energy Hamiltonian is obtained from the spin-orbital superexchange for the triply degenerate  $t_{2g}$  orbitals (Eq. (3.11) from Ref. [19]) by projecting it on the low energy Kramers doublet. In the case of strong spin-orbit coupling, one finds a Heisenberg Hamiltonian for these pseudo-spin-1/2 states, with weak dipolar anisotropy due to Hund's rule coupling. The rotation of the octahedra around the  $z$  axis over an angle  $\alpha \approx 11^\circ$  introduces a Dzyaloshinsky-Moriya interaction, but after an appropriate spin rotation the Hamiltonian remains of Heisenberg type [8].

At the Ir  $L_3$  edge, excitations within the  $J_{\text{eff}} = 1/2$  doublet can be described in terms of Holstein-Primakoff bosons. The single- and double-magnon intensities are,

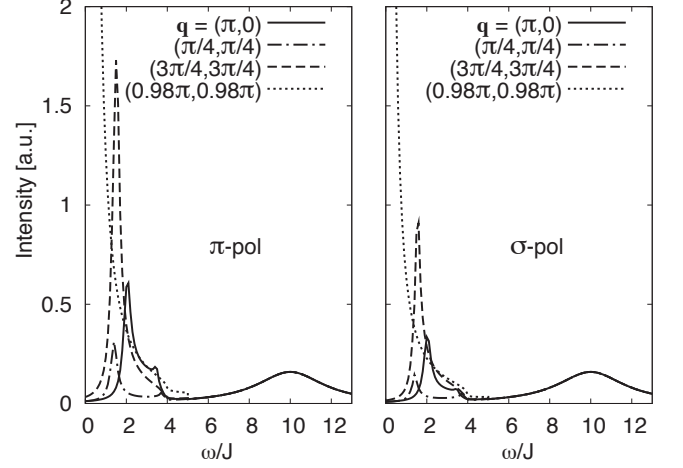


FIG. 2: Vertical cuts through Fig. 1. The left panel shows spectra at several  $\mathbf{q}$  for incoming  $\pi$  polarization, and the right one for incoming  $\sigma$  polarization.

respectively,

$$\begin{aligned}
 I^{(1)} &\propto \left| \frac{\sin \alpha}{\sqrt{2}} (P_x + P_y)(u_{\mathbf{q}} + v_{\mathbf{q}}) - iP_z(u_{\mathbf{q}} - v_{\mathbf{q}}) \right|^2 \\
 &\quad + \frac{1}{2} \cos^2 \alpha |P_x - P_y|^2 (u_{\mathbf{q}} - v_{\mathbf{q}})^2 \delta(\omega - \omega_{\mathbf{q}}), \\
 I^{(2)} &\propto \frac{2}{N} \sum_{\mathbf{k}} \left[ \sin^2 \alpha |P_x - P_y|^2 (u_{\mathbf{k}+\mathbf{q}}v_{\mathbf{k}} + u_{\mathbf{k}}v_{\mathbf{k}+\mathbf{q}})^2 \right. \\
 &\quad \left. + \cos^2 \alpha |P_x + P_y|^2 (u_{\mathbf{k}+\mathbf{q}}v_{\mathbf{k}} - u_{\mathbf{k}}v_{\mathbf{k}+\mathbf{q}})^2 \right] \\
 &\quad \times \delta(\omega - \omega_{\mathbf{k}+\mathbf{q}} - \omega_{\mathbf{k}}), \tag{3}
 \end{aligned}$$

with  $u_{\mathbf{k}} = (1/\sqrt{1 - \gamma_{\mathbf{k}}^2} + 1)^{1/2}/\sqrt{2}$ ,  $v_{\mathbf{k}} = (1/\sqrt{1 - \gamma_{\mathbf{k}}^2} - 1)^{1/2}\text{sign}(\gamma_{\mathbf{k}})/\sqrt{2}$  and  $\gamma_{\mathbf{k}} = (\cos k_x + \cos k_y)/2$ . A remarkable difference with  $L$ -edge RIXS on cuprates [23] is that the large spin canting, reflected in the appreciable value of  $\alpha$ , causes the presence of spectral weight in the center of the Brillouin-zone, at  $\mathbf{q} = \mathbf{0}$ .

Transitions from  $J_{\text{eff}} = 1/2$  to  $3/2$ , which are at an energy of  $\frac{3}{2}\lambda$ , are expected to show a less pronounced  $\mathbf{q}$  dependence. The crystal field splitting of the quartet states is probably too small to resolve with current RIXS instruments, so we give the integrated intensity of all these excitations:  $I^{(g+h)} \propto 2 + |\epsilon' \cdot \epsilon|^2 - |\epsilon'^* \cdot \epsilon|^2$ . The polarization terms cancel unless both incoming and outgoing X-rays are circularly polarized.

*Computed RIXS spectra.* — We now evaluate the different contributions to the RIXS intensity. Single and double magnon contributions  $I^{(1,2)}$  and those from the  $J_{\text{eff}} = 1/2$  to  $3/2$  excitations  $I^{(g+h)}$  are presented for the specific case of a  $90^\circ$  scattering angle with the scattering plane perpendicular to the  $\text{IrO}_2$  layers, and  $\mathbf{q}$  in the first (2D) Brillouin zone. The resulting cross sections are shown in Figs. 1 and 2, where we used  $\frac{3}{2}\lambda/J = 10$ . The

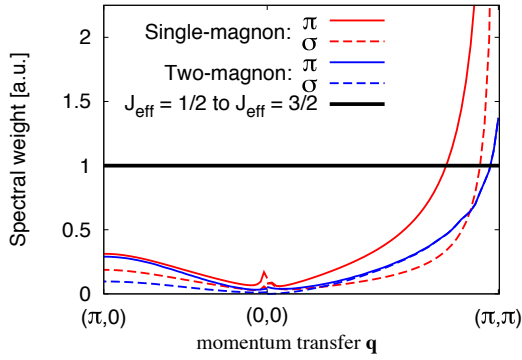


FIG. 3: (Color online.) Spectral weight of different excitations. The units on the vertical axis are chosen such that the  $J_{\text{eff}} = 1/2$  to  $3/2$  excitation has a spectral weight of unity.

low-energy intra doublet excitations with  $\Delta J_{\text{eff}} = 0$  show a very distinct magnon dispersion, the intensity of which is strongly varying with  $\mathbf{q}$ . The doublet-quartet transitions with locally  $\Delta J_{\text{eff}} = 1$  are at  $\frac{3}{2}\lambda$ , corresponding to 0.5 - 0.6 eV [20]. This implies they match in energy the large spectral weight charge modes observed in optical absorption in  $\text{Sr}_2\text{IrO}_4$  [31]. Even if the local multiplet excitations are not optically active themselves, there will be strong mixing of the spin-orbit excited state with inter-site charge excitations across the Mott gap. This causes a delocalization of the doublet-quartet mode on the scale of the intersite hopping  $t$ . The dispersion and momentum dependent spectral weight modulations that this causes is beyond the present model calculations; here it only reflects in the use of an effective broadening of the doublet-quartet mode with  $t$ , corresponding to about  $4J$ .

To summarize, we have determined the effective scattering operators for direct RIXS at the  $L$ -edge of  $\text{Ir}^{4+}$  ions in an octahedral crystal field. In the physical limit of strong spin-orbit coupling, the RIXS spectral weight at the  $L_2$  vanishes, but it is strong at the  $L_3$ -edge. Applying this to  $\text{Sr}_2\text{IrO}_4$ , we find that RIXS can map out the strongly dispersive single- and double-magnon excitations of the low-lying doublet and is in addition sensitive to the doublet-quartet excitations at an energy of  $\frac{3}{2}\lambda$ , which strongly mix with delocalized charge modes. This shows that RIXS can accurately determine the material parameters  $\lambda$  and  $J$  of iridates and is an excellent tool to probe their low-energy elementary excitations, testing and characterizing proposed long-range order and topological phases.

We thank H. Takagi, J. H. Kim, B. J. Kim and M. van Veenendaal for valuable discussions.

- [2] H.A. Jahn and E. Teller, Proc. R. Soc. Lond. A **161**, 220 (1937).
- [3] K.I. Kugel and D.I. Khomskii, Sov. Phys. Usp. **25**, 231 (1982).
- [4] B.J. Kim, H. Ohsumi, T. Komesu, S. Sakai, T. Morita, H. Takagi, and T. Arima, Science **323**, 1329 (2009).
- [5] A. Shitade, H. Katsura, J. Kuneš, X.-L. Qi, S.-C. Zhang, and N. Nagaosa, Phys. Rev. Lett. **102**, 256403 (2009).
- [6] D. Pesin and L. Balents, Nature Physics **6**, 376 (2010).
- [7] J. Chaloupka, G. Jackeli, and G. Khaliullin, Phys. Rev. Lett. **105**, 027204 (2010).
- [8] G. Jackeli and G. Khaliullin, Phys. Rev. Lett. **102**, 017205 (2009).
- [9] A. Kitaev, Ann. Phys. **321**, 2 (2006).
- [10] X. Wan, A. Turner, A. Vishwanath, and S. Y. Savrasov, arXiv:1007.0016 (2010).
- [11] B.-J. Yang and Y. B. Kim, arXiv:1004.4630 (2010).
- [12] C. Cosío-Castaneda, G. Tavizon, A. Baeza, P. de la Mora, and R. Escudero, J. Phys. Cond. Mat. **19**, 446210 (2007).
- [13] Y. Klein and I. Terasaki, J. Phys. Cond. Mat. **20**, 295201 (2008).
- [14] A.V. Powell, P. D. Battle and J. G. Gore, Acta Cryst. C **49**, 852 (1993).
- [15] S. Fujiyama, H. Ohsumi, S. Niitaka, T. Komesu, S. Takeshita, B.J. Kim, T. Arima, and H. Takagi, unpublished.
- [16] A. Kotani and S. Shin, Rev. Mod. Phys. **73**, 203 (2001).
- [17] S. J. Moon *et al.*, Phys. Rev. B **74**, 113104 (2006).
- [18] B. J. Kim *et al.*, Phys. Rev. Lett. **101**, 076402 (2008).
- [19] For a review, see G. Khaliullin, Prog. Theor. Phys. Suppl. **160**, 155 (2005).
- [20] O.F. Schirmer, A.Förster, H. Hesse, M. Wöhlecke, and S. Kapphan, J. Phys. C **17**, 1321 (1984).
- [21] We refer to the cubic axes, parallel to neighboring Ir-Ir bonds. The  $z$  direction is perpendicular to the  $\text{IrO}_2$  plane.
- [22] J. Kanamori, Prog. Theor. Phys. **17**, 177 (1957).
- [23] L.J.P. Ament, G. Ghiringhelli, M. Moretti Sala, L. Braicovich, and J. van den Brink, Phys. Rev. Lett. **103**, 117003 (2009).
- [24] L. Braicovich *et al.*, Phys. Rev. Lett. **104**, 077002 (2010).
- [25] L. Braicovich *et al.*, Phys. Rev. B **81**, 174533 (2010).
- [26] M. Guarise *et al.*, arXiv:1004.2441 (2010).
- [27] L.J.P. Ament, M. van Veenendaal, T.P. Devereaux, J.P. Hill, and J. van den Brink, Rev. Mod. Phys., to be published.
- [28] J.J. Sakurai, *Advanced quantum mechanics* (Addison Wesley, 1967).
- [29] M.O. Krause and J.H. Oliver, J. Phys. Chem. Ref. Data **8**, 329 (1979).
- [30] W. Schülke, *Electron Dynamics by Inelastic X-Ray Scattering* (Oxford University Press, Oxford, 2007).
- [31] S.J. Moon, H. Jin, W.S. Choi, J.S. Lee, S.S.A. Seo, J. Yu, G. Cao, T.W. Noh, and Y.S. Lee, Phys. Rev. B **80**, 195110 (2009).